Author/s:
Ayton, X;Lei, X;Hare, XJ;Duce, JA;George, JL;Adlard, PA;McLean, C;Rogers, JT;Cherny, RA;Finkelstein, DI;Bush, XI

Title:
Parkinson's disease iron deposition caused by nitric oxide- induced loss of β-amyloid precursor protein

Date:
2015-01-01

Citation:
Ayton, X., Lei, X., Hare, X. J., Duce, J. A., George, J. L., Adlard, P. A., McLean, C., Rogers, J. T., Cherny, R. A., Finkelstein, D. I. & Bush, X. I. (2015). Parkinson's disease iron deposition caused by nitric oxide- induced loss of β-amyloid precursor protein. Journal of Neuroscience, 35 (8), pp.3591-3597. https://doi.org/10.1523/JNEUROSCI.3439-14.2015.

Persistent Link:
https://hdl.handle.net/11343/58819

Brief Communications

# Parkinson's Disease Iron Deposition Caused by Nitric Oxide-Induced Loss of β-Amyloid Precursor Protein

Scott Ayton,[1] Peng Lei,[1] Dominic J. Hare,[1,5,6] James A. Duce,[1,2] Jessica L. George,[1] Paul A. Adlard,[1] Catriona McLean,[1,3] Jack T. Rogers,[4] Robert A. Cherny,[1] David I. Finkelstein,[1]* and Ashley I. Bush[1]*

[1]Florey Institute of Neuroscience and Mental Health, University of Melbourne, Parkville, Victoria 3010, Australia, [2]School of Molecular and Cellular Biology, Faculty of Biological Sciences, University of Leeds, Leeds, North Yorkshire, LS2 9JT, United Kingdom, [3]Department of Anatomical Pathology, Alfred Hospital, Prahran, Victoria 3004, Australia, [4]Neurochemistry Laboratory, Department of Psychiatry-Neuroscience, Massachusetts General Hospital (East), Charlestown, Massachusetts 02129, [5]Elemental Bio-imaging Facility, University of Technology Sydney, Broadway, New South Wales, 2007, Australia, and [6]Department of Preventive Medicine, Icahn School of Medicine at Mount Sinai, New York, New York 10029

**Elevation of both neuronal iron and nitric oxide (NO) in the substantia nigra are associated with Parkinson's disease (PD) pathogenesis. We reported previously that the Alzheimer-associated β-amyloid precursor protein (APP) facilitates neuronal iron export. Here we report markedly decreased APP expression in dopaminergic neurons of human PD nigra and that $APP^{-/-}$ mice develop iron-dependent nigral cell loss. Conversely, APP-overexpressing mice are protected in the MPTP PD model. NO suppresses APP translation in mouse MPTP models, explaining how elevated NO causes iron-dependent neurodegeneration in PD.**

*Key words:* **APP; iron; nitric oxide**

## Introduction

Nigral iron elevation in Parkinson's disease (PD) is reported consistently (Oakley et al., 2007; Salazar et al., 2008; Lei et al., 2012; Ayton et al. 2013), affects neurons and glia (Oakley et al., 2007), and is recapitulated in the MPTP model of PD (Lei et al., 2012). Importantly, a selective iron chelator improved PD-motor outcomes in a 12 month randomized clinical trial, achieving a disease-modifying milestone (Devos et al., 2014). Nitrosative stress has also been proposed as a major upstream event in PD pathogenesis (Przedborski et al., 1996; Hung et al., 2012; Chung et al., 2013; Ryan et al., 2013). Nitric oxide (NO) has been linked with iron metabolism (Weiss et al., 1993; Jaffrey et al., 1994) but has not yet been implicated in iron dyshomeostasis in PD.

The Alzheimer's-associated β-amyloid precursor protein (APP) facilitates neuronal iron export through stabilizing cell-surface ferroportin (Duce et al., 2010; McCarthy et al., 2014). Alzheimer- and PD-associated tau protein promotes iron export by trafficking APP to the neuronal surface (Lei et al., 2012). Loss of APP or tau expression causes cellular iron retention (Duce et al., 2010; Lei et al., 2012). Here we explore the role of APP in iron elevation in PD and examine where nitrosative stress fits in the pathogenic sequence.

## Materials and Methods

### *Human brain*

*Bulk tissue study.* Postmortem samples ( processed by the Victoria Brain Bank) from 10 controls (five males) with minimal neuronal pathology and 10 patients (five males) with clinically and pathologically defined PD. The age and postmortem interval were not different between groups. Dissected brain tissue was homogenized in PBS with EDTA-free protease inhibitors (Pierce) and phosphatase inhibitors (Sigma). Iron was measured in homogenate by atomic absorption spectrometry (AAS) as described previously (Ayton et al., 2013). APP (antibody 22C11; in house) was measured by Western blot (4–12% Bis-Tris gels; Invitrogen), corrected for either β-actin (Sigma) or neuron-specific βIII tubulin (Abcam). Antibodies for transferrin receptor 1 (TfR1), divalent metal iron transporter 1 (DMT1) plus iron-responsive element (IRE), and DMT1 without IRE were from Alpha Diagnostics International.

*Laser ablation study.* Sectioned (frozen, 30 μm) postmortem substantia nigra (SN) from four controls (two males) and four PD subjects (one male) were fixed in 4% paraformaldehyde and rinsed repeatedly in PBS before blocking with bovine serum albumin and Triton X-100. Rinsed sections were then incubated overnight in antibody WO2 (Aβ domain of APP). Rinsed sections were then immersed in the blocking solution before 10 min incubation with biotinylated goat anti-mouse IgG. Sections were rinsed and incubated for an additional 10 min with peroxidase-conjugated streptavidin and then enhanced using 3,3′-diaminobenzidine, $Co^{2+}$, and $Ni^{2+}$ (each 0.05% v/v) and rinsed again.

After immunostaining for APP, sections were prepared for tyrosine hydroxylase (TH) labeling with gold nanoparticles following the meth-

Received Aug. 16, 2014; revised Dec. 8, 2014; accepted Jan. 11, 2015.

Author contributions: S.A., P.L., D.J.H., J.A.D., J.L.G., P.A.A., C.M., J.T.R., R.A.C., D.I.F., and A.I.B. designed research; S.A., P.L., D.J.H., J.L.G., and D.I.F. performed research; D.J.H., J.A.D., P.A.A., C.M., J.T.R., R.A.C., and D.I.F. contributed unpublished reagents/analytic tools; S.A., P.L., D.J.H., J.L.G., and A.I.B. analyzed data; S.A., P.L., D.J.H., J.A.D., P.A.A., R.A.C., D.I.F., and A.I.B. wrote the paper.

This work was supported by funds from the Australian Research Council, the Australian National Health and Medical Research Council, the Bethlehem Griffiths Research Foundation, and the Operational Infrastructure Support from the Victorian State Government. The Victorian Brain Bank Network is supported by the University of Melbourne, the Florey Institute of Neuroscience and Mental Health, the Alfred Hospital, and the Victorian Forensic Institute of Medicine.

*D.I.F. and A.I.B. contributed equally to this work.

P.A.A., R.A.C., and D.I.F. are shareholders in and paid scientific consultants for Prana Biotechnology. A.I.B. is a shareholder in Prana Biotechnology, Cogstate, Eucalyptus, Mesoblast, and Brighton Biotech and is a paid consultant for Collaborative Medicinal Developments and Brighton Biotech.

Correspondence should be addressed to Prof. Ashley Bush, Florey Institute of Neuroscience and Mental Health, 30 Royal Parade, Parkville, Victoria 3052, Australia. E-mail: ashley.bush@florey.edu.au.

DOI:10.1523/JNEUROSCI.3439-14.2015

 0270-6474/15/353591-07$15.00/0

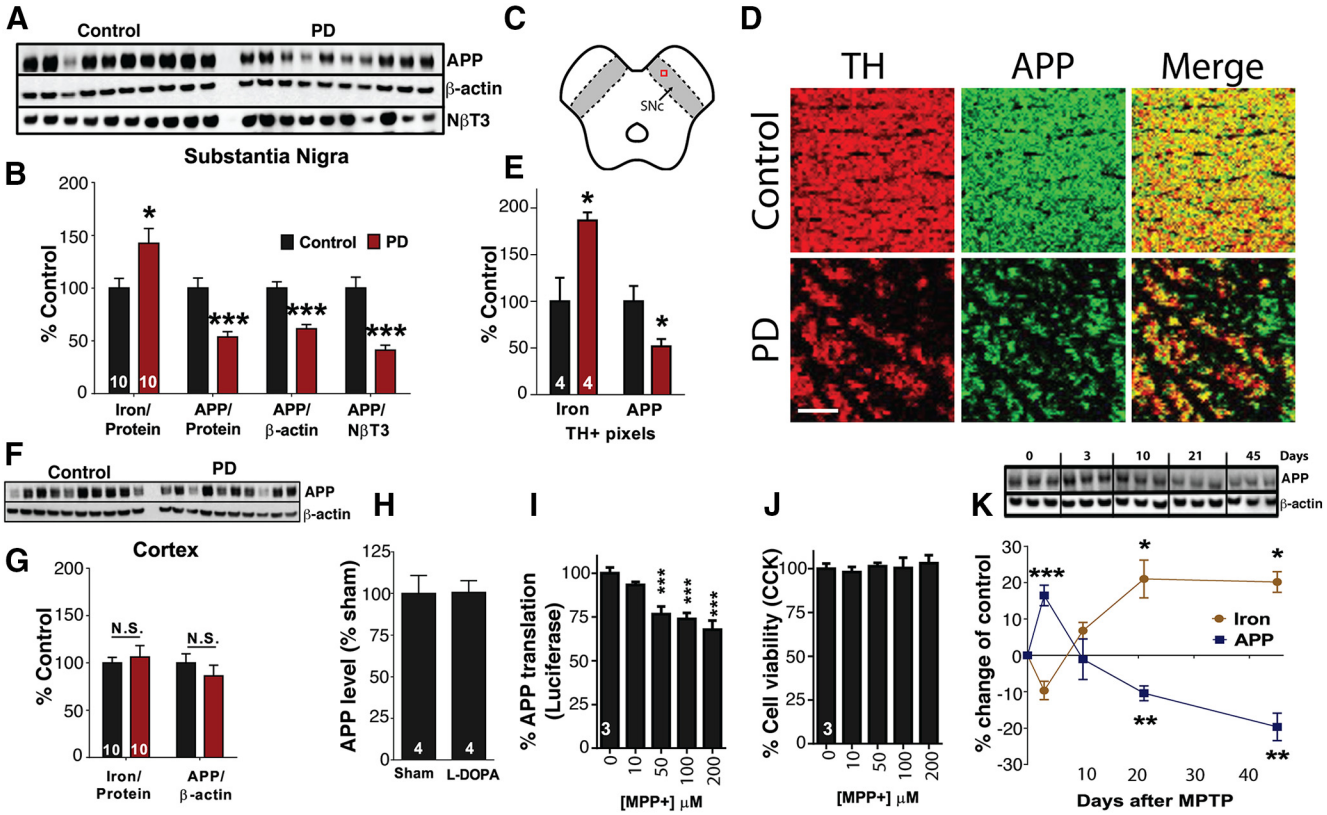


**Figure 1.** Decreased APP expression in PD nigra. ***A–G***, Assay data from postmortem brains of controls and PD patients. ***A***, ***B***, ***F***, ***G***, Homogenized human brain for biochemistry. ***C–E***, Sectioned human SN for LA-ICPMS. ***A***, Western blot for APP levels in SN. ***B***, Iron and APP levels in SN. ***C***, Representative sample area of human SN used for LA-ICPMS analysis. ***D***, Representative LA-ICPMS images of APP (green) and TH (red) content in control and PD sections. Scale bar, 100 $\mu$m. ***E***, LA-ICPMS quantification of APP and iron content in $TH^+$ pixels in sectioned SN of control and PD subjects. ***F***, Western blot for APP levels in the cortex. ***G***, Iron and APP levels in the cortex. ***H***, Nigral APP content in controls and mice administered L-DOPA for 5 months ($n = 4$ each). ***I***, SH-SY5Y cells, transfected with luciferase reporter for APP (IRE-containing) UTR (Rogers et al., 2002), were treated with and without $MPP^+$ (0–200 $\mu$M) for 24 h and then assayed for luminescence (reporting APP translation). Independent experiments indicated in the columns. ***J***, Toxicity assay [cell counting kit (CCK)] performed in parallel to ***I***. ***K***, C57BL/6 mice were injected with MPTP (40 mg/kg) and killed at varying intervals indicated ($n = 10$ each). SN was microdissected and analyzed for iron content and APP levels. Data are means ± SE. $^*p < 0.05$, $^{**}p < 0.01$, $^{***}p < 0.001$ compared with untreated/WT controls. *n* is shown in the graph columns.

ods outlined previously (Hare et al., 2014). Washed and blocked sections were incubated in anti-TH (Millipore). Sections were then rinsed and incubated with goat anti-rabbit IgG preabsorbed with 10 nm gold nanoparticles (Abcam) for 3 h. After an additional three-step rinse with deionized (18.2 MΩ) water, a silver enhancement solution (BBI International) was placed onto the sections and monitored over 30 min. Reduction of metallic silver onto gold nanoparticles was visible as a deep black stain. Rinsed sections were dried before analysis by laser ablation inductively coupled plasma-mass spectrometry (LA-ICPMS).

### *LA-ICPMS imaging*

Imaging of the stained sections was performed using a New Wave Research UP213 laser ablation unit (Kennelec Scientific) and Agilent Technologies 7500cx ICPMS. The UP213 laser emits a frequency-quintupled 213 nm UV laser beam, which was focused into a 12-$\mu$m-diameter spot with an energy fluence of 0.3 $J/cm^{-2}$. An average of 11,300 pixels were sampled per brain slice. Brain slices were placed within a two-volume large format ablation cell (New Wave Research). Signal response was normalized against repeated calibration of matrix-matched tissue standards (Hare et al., 2014). Argon was used as a carrier gas. The Agilent 7500cx ICPMS was retrofitted with a "cs" lens system for enhanced sensitivity. Masses (mass/charge ratio) measured included 59 (cobalt), 60 (nickel), 107 (silver), 197 (gold), and 56 (iron). Standard ICPMS operating parameters were as reported previously (Hare et al., 2014).

On completion of analysis, data were exported from the ChemStation software (Agilent) and analyzed using ENVI (Exelis Visual Information Solutions). Images for cobalt were used to represent APP distribution and gold for TH. After background correction, images were divided into TH-positive ($TH^+$) and TH-negative regions, and APP levels in $TH^+$ areas were extracted as counts per second of cobalt, per pixel, per section.

### *Dopamine*

Striatal dopamine was measured using HPLC with electrochemical detection as described previously (Duce et al., 2013).

### *Mice*

Mice were housed in a conventional animal facility and fed non-meat chow from Specialty Feeds. MPTP doses were chosen (40–60 mg/kg) to minimize animal deaths. At the conclusion of each experiment, mice were transcardially perfused with ice-cold PBS under deep anesthesia (sodium pentobarbitone, 100 mg/kg).

Animal performance studies were performed as described previously (Lei et al., 2012)

*MPTP time course.* C57BL/6 male mice administered MPTP (4 × 10 mg/kg, i.p., 2 h intervals) were killed on the days indicated and compared with untreated littermates. Microdissected SN was homogenized in PBS with protease inhibitors. APP (22C11, corrected for $\beta$-actin) and iron (AAS) was measured.

*$APP^{-/-}$ deferiprone trial.* Deferiprone (DFP; Sigma) was administered in drinking water to 3-month-old $APP^{-/-}$ mice ($50\ mg \cdot kg^{-1} \cdot d^{-1}$) for 3 months. These were compared with age-matched untreated $APP^{-/-}$ and wild-type (WT; C57BL/6/129Sv) mice. The midbrain was sectioned for stereological estimation of Nissl-stained SN neurons according to our previous protocols (Ayton et al., 2013).

*Tg2576/MPTP trial.* Four-month-old Tg2576 and littermate background control C57BL/6/SJL (WT) mice administered MPTP (4 × 10 or

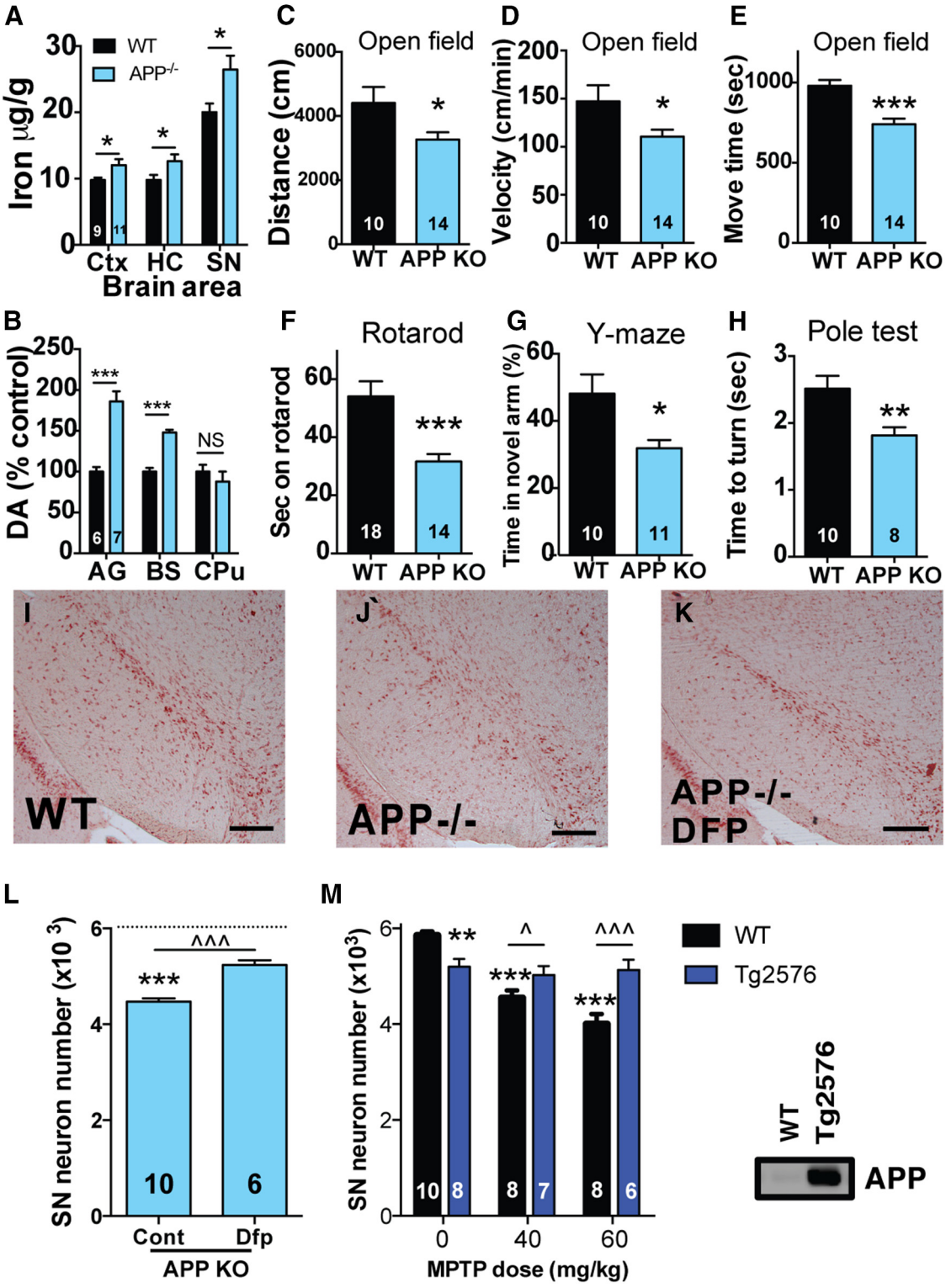


**Figure 2.** APP protects against nigral neuron loss. ***A***, Iron content in the cortex (Ctx), hippocampus (HC), and SN from WT and $APP^{-/-}$ mice. ***B***, Dopamine (DA) content in the adrenal gland (AG), brainstem (BS), and caudate–putamen (CPu) from WT and $APP^{-/-}$ mice. ***C–E***, Reduced motor performance of $APP^{-/-}$ mice in open-field measures of distance moved (***C***), velocity (***D***), and time in movement (***E***). SNc, Substantia nigra pars compacta. ***F***, Impaired cognitive performance of $APP^{-/-}$ mice in the Y-maze. ***H***, Improved pole test performance in $APP^{-/-}$ mice. ***J–L***, WT and $APP^{-/-}$ mice were aged to 6 months before analysis. A subgroup of $APP^{-/-}$ mice were treated with DFP from 3 months of age. SN neuron number was estimated by stereology, with representative images (scale bar, 250 $\mu$m) shown in ***I–K*** and counts displayed in ***L***. Cont, Control. ***M***, Nigral neuron counts of APP overexpressing (Tg2576) and WT mice treated with and without MPTP and killed at 21 d. Data are means ± SE. $^{*}p < 0.05$, $^{**}p < 0.01$, $^{***}p < 0.001$ compared with untreated, WT controls. $^{\wedge}p < 0.05$, $^{\wedge\wedge\wedge}p < 0.001$ as indicated. *n* is shown in the graph columns.

3 × 20 mg/kg every 2 h) were killed after 21 d. The midbrain was removed for stereological estimation of Nissl-stained SN neurons.

*7-Nitroindazole chronic treatment trial.* Five-month-old C57BL/6 male mice were administered 7-nitroindazole (7-NI; 50 mg/kg, i.p.) every 3 d for 21 d. Microdissected SN was removed and assayed for iron (AAS) and APP (Western blot, antibody 22C11).

*7-NI/MPTP trial.* Six-month-old *APP*$^{-/-}$ mice and WT littermates were administered 7-NI (50 mg/kg in peanut oil, i.p.) and/or MPTP (4 × 10 mg/kg, i.p. every 2 h). Separate controls were intoxicated with MPTP and then treated with the monoamine oxidase B (MAO-B) inhibitor selegiline (50 mg/kg in saline, i.p.), in the same dosing regimen as 7-NI-treated mice. Treatment began 24 h after MPTP and was then repeated for the next 2 d and then once every 3 d thereafter. Mice were killed after 21 d, their right SN was sectioned for stereology, and the left SN was removed for Western blot (22C11) and iron analysis (AAS).

### *Tissue culture*

*M17 cells.* BE(2)–M17 human neuroblastoma cells were treated with diethylenetriamine NONOate (DETA-NONOate; 100 μM; Sigma) for 24 h and lysate assayed for APP (antibody WO2) and iron (AAS).

*APP–luciferase expression.* SH-SY5Y cells were transfected as reported previously (Rogers et al., 2002). After 5 h of MPP$^+$ (100 μM; Sigma) and L-NAME (100 μM; Sigma) treatment, media were removed with lysis buffer (Promega) and added to luciferase assay reagent (Promega), and luminescence was recorded (Flexstation 3; Molecular Devices).

### *IRE binding assay*

We modified our previous assay of APP mRNA–biotin binding to iron-responsive protein-1 (IRP1; Duce et al., 2010) using streptavidin-conjugated M-280 Dynabeads (Invitrogen) to test the effect of exogenous NO. Two hundred micrograms of protein from SY5Y lysate [in 25 mM Tris, 0.5% NP-40, 0.5% Triton X-100, 15 mM NaCl, EDTA-free protease inhibitors (Pierce), and SUPERase RNase inhibitor (Life Technologies)] were precleared with 5 μl Dynabeads. Cell lysate (200 μg protein/condition) with or without 100 nM biotin–APP mRNA [APP IRE (5-biotin-GC GGU GGC GGC GCG GGC AGA GCA AGG ACG CGG CGG AU-3) or biotin–APPmut mRNA (5-biotin-GC GGU GGC GGC GCG GG(C AGA) GCA AGG ACG CGG CGG AU-3] was incubated for 3 h at room temperature. DETA-NONOate (100 μM; Sigma) was then added to one preparation containing WT APP mRNA, and all lysates were incubated for an additional 1 h at room temperature. Washed beads were eluted and probed for IRP1.

## Results

### Loss of APP engenders vulnerability to PD

We examined postmortem PD and control SN tissue ($n$ = 10 each) and found

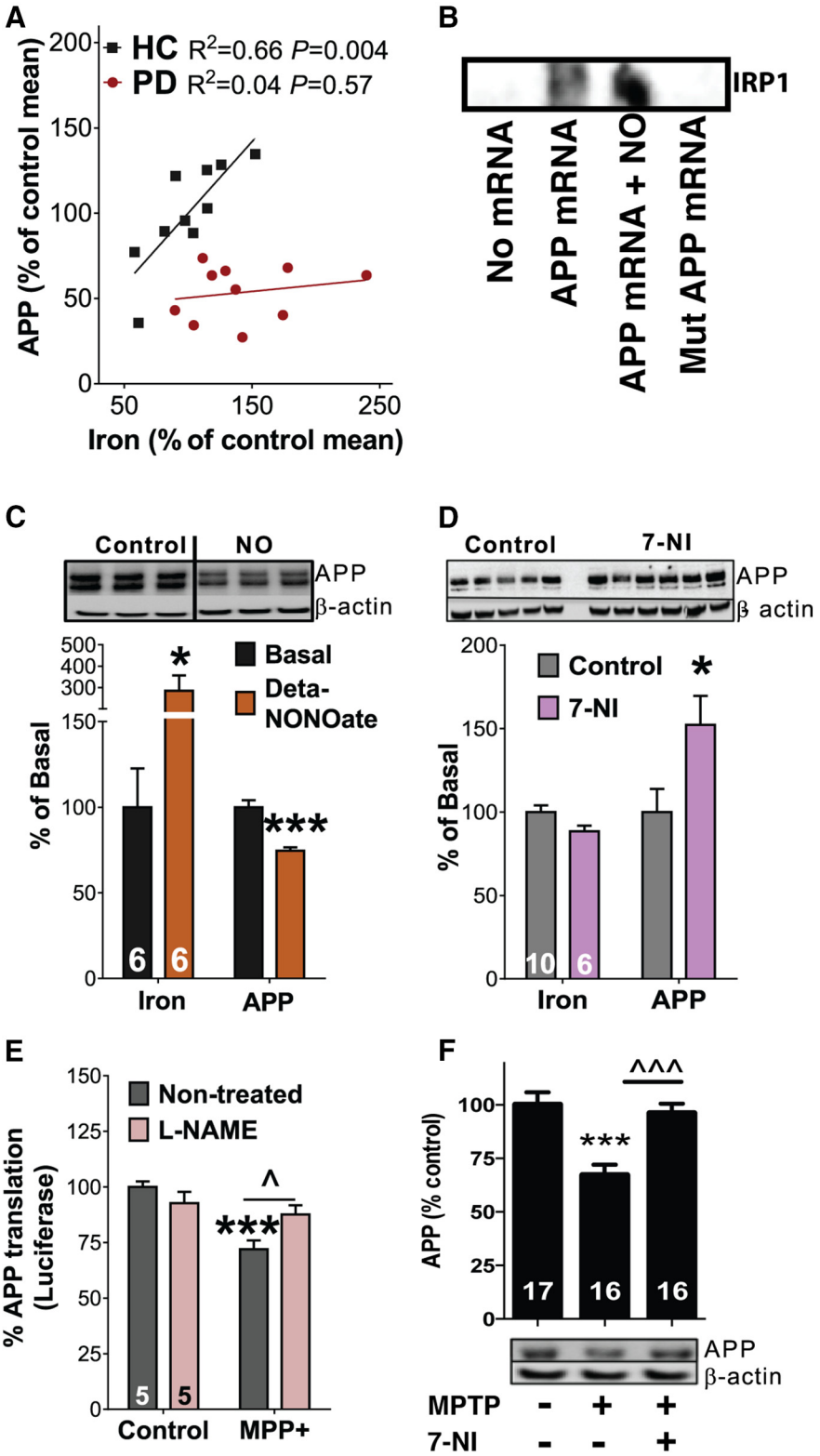


**Figure 3.** NO lowers APP translation. ***A***, Pearson's correlation between nigral iron and APP content in control and PD brains. ***B***, Biotinylated APP mRNA and APPmut mRNA was used to pull down IRP1 from SY5Y cell homogenate. IRP1 binding was increased in the presence of the NO donor DETA-NONOate. ***C***, Iron and APP levels in M17 control cells and cells treated for 24 h with the NO donor DETA-NONOate (100 μM). ***D***, Iron and APP levels in SN of control mice and mice treated with 7-NI over 21 d. ***E***, SH-SY5Y cells, transfected with luciferase reporter for APP (IRE-containing) UTR (Rogers et al., 2002), were treated with or without MPP$^+$ (100 μM) and with or without L-NAME (100 μM) for 24 h and then assayed for luminescence (reporting APP translation). Independent experiments indicated in the columns. ***F***, WT mice treated with and without MPTP were compared with mice cotreated with 7-NI over 21 d. Nigral APP levels in SN from different treatment groups were measured by Western blot. Data are means ± SE. *$p < 0.05$, ***$p < 0.001$ compared with untreated/WT controls. ^$p < 0.05$, ^^^$p < 0.001$ as indicated. $n$ is shown in the graph columns.

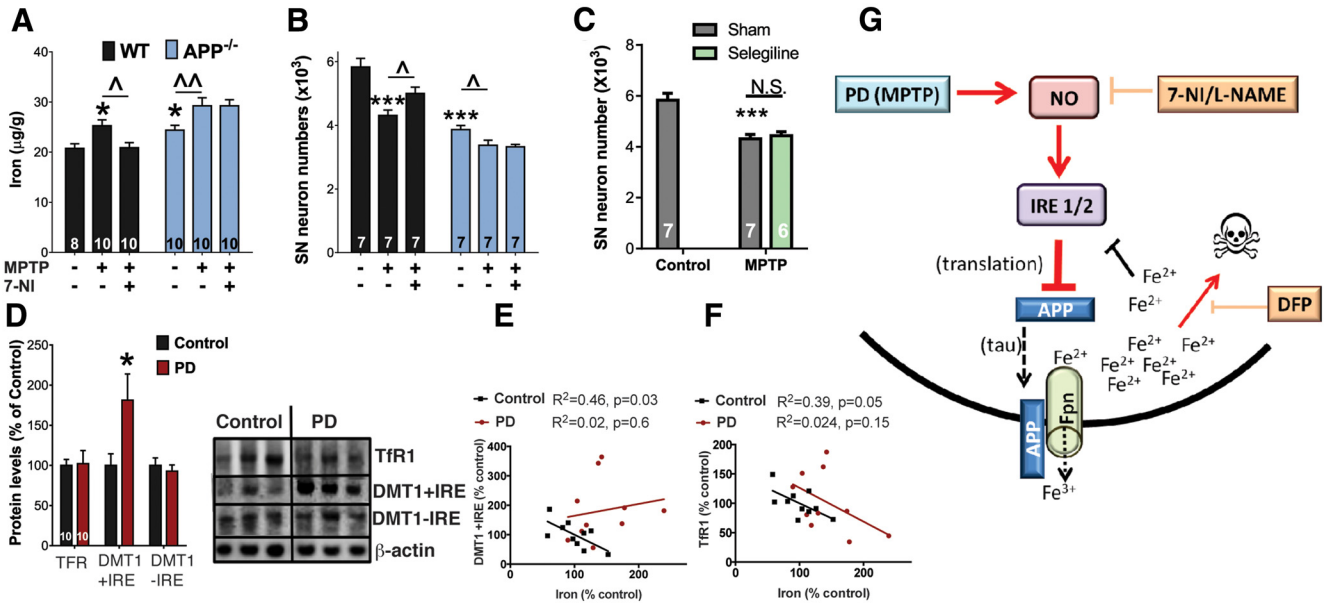


**Figure 4.** Inhibition of APP translation by NO causes iron elevation in PD. ***A***, ***B***, WT and APP knock-out mice treated with and without MPTP were compared with mice cotreated with 7-NI. ***A***, Nigral iron content. ***B***, Nigral neuron count (stereology). ***C***, SN neuron counts of WT mice administered MPTP and then treated with or without selegiline. ***D***, SN of control and PD patients were assayed for TfR1, DMT1 + IRE, and DMT1 − IRE. ***E***, ***F***, Pearson's correlations between nigral iron and DMT1 + IRE (***E***) and TfR1 (***F***) in control and PD brains. ***G***, Model: Elevated NO in PD depresses APP translation by promoting IRP binding to the IRE on 5′UTR. Iron accumulates as a result of reduced APP-mediated iron export. Drugs that inhibit NO elevation (7-NI/L-NAME) or remove excess iron (DFP) confer neuroprotection. Data are means ± SE. $*p < 0.05$, $***p < 0.001$ compared with untreated/WT controls. $\hat{}p < 0.05$, $\hat{}\hat{}\hat{}p < 0.001$ as indicated. *n* is shown in the graph columns.

lower APP protein levels in PD cases (Fig. 1*A*,*B*), whether this was corrected for total protein (−46%; *t* test, $p < 0.001$), β-actin (−39%; *t* test, $p < 0.001$), or neuron-specific β-tubulin III (−59%; *t* test, $p < 0.001$). We then interrogated APP levels specifically in $TH^+$ neurons of sectioned SN postmortem samples of a different patient cohort (four controls and four with PD; Fig. 1*C*) using LA-ICPMS (Hare et al., 2014). We mapped nigral TH and APP immunoreactivities at 12 μm resolution (Fig. 1*D*), and, as expected, there was a conspicuous decrease in $TH^+$ pixel density in the PD cases (Fig. 1*C*,*D*). Even so, we found that the average APP content in $TH^+$ pixels was 50% less in PD subjects compared with controls ($p = 0.05$; Fig. 1*E*), confirming that loss of APP in this region is not merely attributable to loss of TH neurons but, rather, the neurons are expressing less APP.

APP loss impairs iron efflux (Duce et al., 2010), and accordingly, iron was elevated in homogenized SN tissue of PD patients (42%; *t* test, $p = 0.014$; Fig. 1*B*) as observed previously (Ayton et al., 2013). Using LA-ICPMS, we found that this elevation was predominantly attributable to iron accumulation in dopaminergic neurons because iron content in $TH^+$ pixels of PD SN sections was increased by 90% ($p = 0.018$; Fig. 1*E*). APP and iron levels were unaltered in the cortex of the original patient cohort (Fig. 1*F*,*G*). APP loss in PD is not likely to be attributable to L-DOPA therapy because chronic treatment did not change nigral APP levels in mice (Fig. 1*H*). The postmortem interval was not significantly different between groups and not likely to account for loss of nigral APP because cortical tissue from the same cohort was not decreased.

We next investigated whether APP loss occurs in the neuronal culture and mouse MPTP models of PD. First, we studied SH-SY5Y neuroblastoma cells transfected with a luciferase reporter flanked by the IRE-containing 5′UTR of APP (Rogers et al., 2002) and found that $MPP^+$ (active metabolite of MPTP) suppressed APP translation (Fig. 1*I*) at concentrations that did not cause toxicity (Fig. 1*J*). Similarly, in the MPTP mouse model of PD, nigral APP loss also was observed 21 d after intoxication, coincident with iron elevation, as we showed previously (Lei et al., 2012; Fig. 1*K*).

Because decreased nigral APP is a feature of both PD and PD models, we explored whether $APP^{-/-}$ mice express aspects of a PD phenotype. Six-month-old $APP^{-/-}$ mice exhibited iron elevation in SN (32%; *t* test, $p = 0.021$), and, consistent with our previous findings (Duce et al., 2010), iron was also elevated in the cortex (23%; *t* test, $p = 0.044$) and hippocampus (29%; *t* test, $p = 0.043$; Fig. 2*A*). So, the iron phenotype for $APP^{-/-}$ mice is not specifically parkinsonian in its anatomical distribution. We also reported recently that $APP^{-/-}$ mice have elevated catecholamines, including dopamine, in their brains and in the periphery (Duce et al., 2013). We found in this series of animals that $APP^{-/-}$ mice express elevated dopamine in the adrenal gland (85%; *t* test, $p = 0.029$) and brainstem (48%; *t* test, $p = 0.006$), as shown previously, but striatal levels were unaltered (−12%; *t* test, $p = 0.45$; Fig. 2*B*).

Although the dopamine findings are not consistent with advanced human PD, $APP^{-/-}$ mice are known to exhibit motor disability (Zheng et al., 1995), which we confirmed using the open-field (Fig. 2*C–E*) and rotarod (Fig. 2*F*) assays. We also found that $APP^{-/-}$ mice are impaired cognitively in the Y maze (*t* test, $p = 0.014$; Fig. 2*G*). $APP^{-/-}$ mice were not impaired in the pole test (Fig. 2*H*); therefore, the motor phenotype is not fully penetrant.

If APP loss leads to toxic iron elevation in PD, then $APP^{-/-}$ mice should also exhibit nigral neurodegeneration. We found moderate nigral neuron loss in 6-month-old $APP^{-/-}$ mice (−27%; two-factor ANOVA, $p < 0.001$; Fig. 2*I–L*), which could be consistent with the partial motor phenotype of $APP^{-/-}$ mice, but we do not exclude the possibility that degeneration to other regions contributes to the motor phenotype. Indeed, dopamine is not decreased in 6-month-old $APP^{-/-}$ mice, which is evidence for extranigral genesis of motor dysfunction. However, the data demonstrate that loss of APP is a sufficient cause of significant

nigral neuron loss; therefore, low APP levels in PD could potentially contribute to neurodegeneration. In addition, low APP causing higher dopamine levels might explain the conservation of striatal dopamine levels as compensation of SN neuronal loss in PD (Arkadir et al., 2014).

To confirm that neuronal degeneration in $APP^{-/-}$ mice was caused by an iron-dependent mechanism, we treated 3-month-old $APP^{-/-}$ mice with the iron chelator DFP for 3 months and found that treatment ameliorated SN loss (preventing ~50% neuron loss; $p < 0.001$; Fig. 2*I–L*).

To further test the importance of APP expression in protecting the nigra against neurodegeneration, we tested whether APP overexpression might protect against MPTP. Indeed, Tg2576 mice (an APP overexpressing model of AD) were resistant to MPTP-induced SN neuronal loss (two-factor ANOVA, Dunnett's *post hoc* test, $p = 0.05$ at 40 mg/kg; $p < 0.001$ at 60 mg/kg; Fig. 2*M*). Consistent with previous observations of catecholaminergic neuronal loss in this AD model (Guérin et al., 2009), minor SN neuronal loss (−10%; $p = 0.005$) was evident in nontreated Tg2576 controls (Fig. 2*M*).

### NO dysregulates APP translation

What could cause APP loss in PD? IRP1/2 regulate APP translation through a 5′UTR IRE in APP mRNA (Rogers et al., 2002). When iron is replete, IRP1/2 protein are blocked from binding to APP IRE, disinhibiting the translation of the protein. If nigral iron elevation was upstream in PD pathogenesis, APP expression would be elevated, but because APP is decreased in this tissue (Fig. 1*A–E*), APP expression might be suppressed by an upstream lesion. Consistent with this possibility, the correlation of APP with iron levels in normal SN ($r^2 = 0.66$, $p = 0.004$; reflecting IRE-dependent translation) was lost in PD ($r^2 = 0.042$, $p = 0.6$; Fig. 3*A*).

NO increases binding between IRP1/2 and IREs, inappropriately simulating iron deprivation (Weiss et al., 1993; Jaffrey et al., 1994). Indeed, biotyinlated APP mRNA pull down of IRP1 from cell lysate was enhanced by coincubation with the NO donor DETA-NONOate (Fig. 3*B*). Therefore, we hypothesized that APP expression could be suppressed by NO in PD, in which NO is elevated (Przedborski et al., 1996). Indeed, the NO donor DETA-NONOate suppressed APP expression (−25%; $p < 0.001$) and induced marked iron accumulation in M17 neuroblastoma cells (Fig. 3*C*). Conversely, long-term treatment of mice with the NO synthase (NOS) inhibitor 7-NI increased nigral APP levels (50%; *t* test, $p = 0.035$; Fig. 3*D*). These results are consistent with the elevation of APP expression observed in brain and other tissue of $eNOS^{-/-}$ mice (Austin et al., 2010). Therefore, excess NO could cause iron retention in PD by inappropriately suppressing APP expression.

We examined this mechanism in two PD models. First, in luciferase-transfected SH-SY5Y cells, we found that the $MPP^+$-induced suppression of APP translation (Fig. 1*I,J*) was rescued by the water-soluble NOS inhibitor L-NAME (Fig. 3*E*). In mice, NOS inhibition with 7-NI, shown previously to ameliorate MPTP neurotoxicity (Przedborski et al., 1996; Di Monte et al., 1997), reversed the suppression of nigral APP induced by MPTP intoxication of mice (ANOVA, $p < 0.001$; Fig. 3*F*). Consistent with rescuing APP expression, 7-NI also prevented the associated nigral iron elevation (20%; two-factor ANOVA, Dunnett's *post hoc* test, $p = 0.013$; Fig. 4*A*) and accompanying neuronal loss (rescued ~50%, two-factor ANOVA, Dunnett's *post hoc* test, $p = 0.018$; Fig. 4*B*). 7-NI was unable to rescue MPTP-induced iron accumulation or neuronal loss in $APP^{-/-}$ mice (Fig. 4*A,B*), demonstrating that 7-NI relieves toxic iron accumulation in WT mice by increasing APP expression that is otherwise suppressed by NO.

7-NI has been shown to inhibit MAO-B, which could be neuroprotective by preventing MPTP oxidation into toxic $MPP^+$ (Di Monte et al., 1997). To control for this, the 7-NI was only delivered 24 h after MPTP intoxication (to ensure the MPTP has been fully oxidized). We also tested a more potent MAO-B inhibitor, selegiline, and found that it was not neuroprotective when used in an identical dosing regimen, delivered 24 h after MPTP (Fig. 4*C*).

Iron accumulation could also be contributed by increased iron import through the TfR1 and DMT1 pathways. 3′UTR IREs regulate translation of TfR1 and an isoform of DMT1 (DMT1 + IRE) but not an alternate isoform that does not have an IRE (DMT1 − IRE). The effect of iron elevation on the 3′UTR IREs is to suppress levels of TfR1 and DMT1 + IRE, in contrast to the effect of iron on APP translation. However, TfR1 and DMT1 levels were not suppressed despite elevated nigral iron in PD SN samples (Fig. 4*D*), which is consistent with previous reports (Morris et al., 1994; Salazar et al., 2008). Like APP, the significant associations between iron and both DMT1 + IRE ($r^2 = 0.46$; Fig. 4*E*) and TfR1 ($r^2 = 0.40$; Fig. 4*F*) in control nigral tissue were also lost in PD tissue. Together, our findings indicate broadly dysregulated iron sensing by IRP1/2 in PD nigra.

## Discussion

Here we show that iron retention in PD SN is contributed to by impaired iron export attributable to loss of APP expression (Fig. 1), mediated by upstream NO elevation (Fig. 3). In iron-replete conditions (as in PD), IRP should release IREs on target mRNA, leading to elevated APP and decreased TfR1 and DMT1 expression. The opposite shift in these proteins observed in PD nigra (Figs. 1*A–E*, 4*D–F*) indicates pathologically dysregulated iron sensing. We found that NO mimics iron deprivation and inappropriately suppresses APP translation (Fig. 3*B,C*). Loss of APP translation in PD leads to iron retention (Fig. 1*A,E*) and decouples the normal APP response to nigral iron elevation (Fig. 3*A*). In PD models, inhibition of NO corrected the loss of APP (Fig. 3*E,F*). Therefore, our findings mechanistically sequence elevated NO as causatively upstream of nigral iron elevation in PD (Fig. 4*G*). The mechanism we describe illuminates new therapeutic avenues to target iron overload in PD. Our findings indicate that NO scavengers, such as Cu(II)ATSM [diacetylbis(*N*(4)-methylthiosemicarbazonato) copper(II)], which have shown benefit in multiple PD models (Hung et al., 2012), may also act to lower toxic iron accumulation.

## References

Arkadir D, Bergman H, Fahn S (2014) Redundant dopaminergic activity may enable compensatory axonal sprouting in Parkinson disease. Neurology 82:1093–1098. CrossRef Medline

Austin SA, Santhanam AV, Katusic ZS (2010) Endothelial nitric oxide modulates expression and processing of amyloid precursor protein. Circ Res 107:1498–1502. Medline

Ayton S, Lei P, Duce JA, Wong BX, Sedjahtera A, Adlard PA, Bush AI, Finkelstein DI (2013) Ceruloplasmin dysfunction and therapeutic potential for parkinson disease. Ann Neurol 73:554–559. Medline

Chung CY, Khurana V, Auluck PK, Tardiff DF, Mazzulli JR, Soldner F, Baru V, Lou Y, Freyzon Y, Cho S, Mungenast AE, Muffat J, Mitalipova M, Pluth MD, Jui NT, Schüle B, Lippard SJ, Tsai LH, Krainc D, Buchwald SL, Jaenisch R, Lindquist S (2013) Identification and rescue of alpha-synuclein toxicity in Parkinson patient-derived neurons. Science 342:983–987. CrossRef Medline

Devos D, Moreau C, Devedjian JC, Kluza J, Petrault M, Laloux C, Jonneaux A, Ryckewaert G, Garçon G, Rouaix N, Duhamel A, Jissendi P, Dujardin K, Auger F, Ravasi L, Hopes L, Grolez G, Firdaus W, Sablonnière B, Strubi-

Vuillaume I, Zahr N, Destée A, Corvol JC, Pöltl D, Leist M, Rose C, Defebvre L, Marchetti P, Cabantchik ZI, Bordet R (2014) Targeting chelatable iron as a therapeutic modality in Parkinson's disease. Antioxid Redox Signal 21:195–210. CrossRef Medline

Di Monte DA, Royland JE, Anderson A, Castagnoli K, Castagnoli N Jr, Langston JW (1997) Inhibition of monoamine oxidase contributes to the protective effect of 7-nitroindazole against MPTP neurotoxicity. J Neurochem 69:1771–1773. Medline

Duce JA, Tsatsanis A, Cater MA, James SA, Robb E, Wikhe K, Leong SL, Perez K, Johanssen T, Greenough MA, Cho HH, Galatis D, Moir RD, Masters CL, McLean C, Tanzi RE, Cappai R, Barnham KJ, Ciccotosto GD, Rogers JT, Bush AI (2010) Iron-export ferroxidase activity of beta-amyloid precursor protein is inhibited by zinc in Alzheimer's disease. Cell 142:857–867. CrossRef Medline

Duce JA, Ayton S, Miller AA, Tsatsanis A, Lam LQ, Leone L, Corbin JE, Butzkueven H, Kilpatrick TJ, Rogers JT, Barnham KJ, Finkelstein DI, Bush AI (2013) Amine oxidase activity of beta-amyloid precursor protein modulates systemic and local catecholamine levels. Mol Psychiatry 18:245–254. Medline

Guérin D, Sacquet J, Mandairon N, Jourdan F, Didier A (2009) Early locus coeruleus degeneration and olfactory dysfunctions in Tg2576 mice. Neurobiol Aging 30:272–283. Medline

Hare DJ, Lei P, Ayton S, Roberts BR, Grimm R, George JL, Bishop D, Beavis A, Donovan SJ, McColl G, Volitakis I, Masters CL, Adlard PA, Cherny RA, Bush AI, Finkelstein DI, Doble P (2014) An iron-dopamine index predicts risk of parkinsonian neurodegeneration in the substantia nigra pars compacta. Chem Sci 5:2160–2169. CrossRef

Hung LW, Villemagne VL, Cheng L, Sherratt NA, Ayton S, White AR, Crouch PJ, Lim S, Leong SL, Wilkins S, George J, Roberts BR, Pham CL, Liu X, Chiu FC, Shackleford DM, Powell AK, Masters CL, Bush AI, O'Keefe G, Culvenor JG, Cappai R, Cherny RA, Donnelly PS, Hill AF, Finkelstein DI, Barnham KJ (2012) The hypoxia imaging agent CuII(atsm) is neuroprotective and improves motor and cognitive functions in multiple animal models of Parkinson's disease. J Exp Med 209:837–854. Medline

Jaffrey SR, Cohen NA, Rouault TA, Klausner RD, Snyder SH (1994) The iron-responsive element binding protein: a target for synaptic actions of nitric oxide. Proc Natl Acad Sci USA 91:12994–12998. CrossRef Medline

Lei P, Ayton S, Finkelstein DI, Spoerri L, Ciccotosto GD, Wright DK, Wong BX, Adlard PA, Cherny RA, Lam LQ, Roberts BR, Volitakis I, Egan GF, McLean CA, Cappai R, Duce JA, Bush AI (2012) Tau deficiency induces parkinsonism with dementia by impairing APP-mediated iron export. Nat Med 18:291–295. Medline

McCarthy RC, Park YH, Kosman DJ (2014) sAPP modulates iron efflux from brain microvascular endothelial cells by stabilizing the ferrous iron exporter ferroportin. EMBO Rep 15:809–815. CrossRef Medline

Morris CM, Candy JM, Omar S, Bloxham CA, Edwardson JA (1994) Transferrin receptors in the parkinsonian midbrain. Neuropathol Appl Neurobiol 20:468–472. Medline

Oakley AE, Collingwood JF, Dobson J, Love G, Perrott HR, Edwardson JA, Elstner M, Morris CM (2007) Individual dopaminergic neurons show raised iron levels in Parkinson disease. Neurology 68:1820–1825. CrossRef Medline

Przedborski S, Jackson-Lewis V, Yokoyama R, Shibata T, Dawson VL, Dawson TM (1996) Role of neuronal nitric oxide in 1-methyl-4-phenyl-1,2,3,6-tetrahydropyridine (MPTP)-induced dopaminergic neurotoxicity. Proc Natl Acad Sci USA 93:4565–4571. CrossRef Medline

Rogers JT, Randall JD, Cahill CM, Eder PS, Huang X, Gunshin H, Leiter L, McPhee J, Sarang SS, Utsuki T, Greig NH, Lahiri DK, Tanzi RE, Bush AI, Giordano T, Gullans SR (2002) An iron-responsive element type II in the 5′-untranslated region of the Alzheimer's amyloid precursor protein transcript. J Biol Chem 277:45518–45528. Medline

Ryan SD, Dolatabadi N, Chan SF, Zhang X, Akhtar MW, Parker J, Soldner F, Sunico CR, Nagar S, Talantova M, Lee B, Lopez K, Nutter A, Shan B, Molokanova E, Zhang Y, Han X, Nakamura T, Masliah E, Yates JR 3rd, Nakanishi N, Andreyev AY, Okamoto S, Jaenisch R, Ambasudhan R, Lipton SA (2013) Isogenic human iPSC Parkinson's model shows nitrosative stress-induced dysfunction in MEF2-PGC1alpha transcription. Cell 155:1351–1364. CrossRef Medline

Salazar J, Mena N, Hunot S, Prigent A, Alvarez-Fischer D, Arredondo M, Duyckaerts C, Sazdovitch V, Zhao L, Garrick LM, Nuñez MT, Garrick MD, Raisman-Vozari R, Hirsch EC (2008) Divalent metal transporter 1 (DMT1) contributes to neurodegeneration in animal models of Parkinson's disease. Proc Natl Acad Sci USA 105:18578–18583. CrossRef Medline

Weiss G, Goossen B, Doppler W, Fuchs D, Pantopoulos K, Werner-Felmayer G, Wachter H, Hentze MW (1993) Translational regulation via iron-responsive elements by the nitric oxide/NO-synthase pathway. EMBO J 12:3651–3657. Medline

Zheng H, Jiang M, Trumbauer ME, Sirinathsinghji DJ, Hopkins R, Smith DW, Heavens RP, Dawson GR, Boyce S, Conner MW, Stevens KA, Slunt HH, Sisoda SS, Chen HY, Van der Ploeg LH (1995) beta-Amyloid precursor protein-deficient mice show reactive gliosis and decreased locomotor activity. Cell 81:525–531. CrossRef Medline